The Journal of Experimental Biology 208, 4727-4733
Published by The Company of Biologists 2005
doi:10.1242/jeb.01933

Analysis of the effects of turning bias on chemotaxis in *C. elegans*

Jonathan T. Pierce-Shimomura[1,2,*], Michael Dores[2] and Shawn R. Lockery[2]

[1]*Ernest Gallo Clinic and Research Center, Department of Neurology, Programs in Neuroscience and Biomedical Science, University of California, San Francisco, 5858 Horton Street, Suite 200, Emeryville, CA 94608, USA* and [2]*Institute of Neuroscience, University of Oregon, Eugene, OR 97403-1254, USA*

*Author for correspondence (e-mail: jonp@egcrc.net)

Accepted 17 October 2005

Summary

C. elegans **advances up a chemical gradient by modulating the probability of occasional large, course-correcting turns called pirouettes. However, it remains uncertain whether *C. elegans* also uses other behavioral strategies for chemotaxis. Previous observations of the unusual, spiral-shaped chemotaxis tracks made by the bent-head mutant *unc-23* point to a different strategy in which the animal continuously makes more subtle course corrections. In the present study we have combined automated tracking of individual animals with computer modeling to test the hypothesis that the pirouette strategy is sufficient on its own to account for the spiral tracks. Tracking experiments showed that the bent-head phenotype causes a strong turning bias and disrupts pirouette execution but does not disrupt pirouette initiation. A computer simulation of disrupted pirouette behavior and turning bias reproduced the spiral tracks of *unc-23* chemotaxis behavior, showing that the pirouette strategy is sufficient to account for the mutant phenotype. In addition, the simulation reproduced higher order features of the behavior such as the relationship between the handedness of the spiral and the side to which the head was bent. Our results suggest that the pirouette mechanism is sufficient to account for a diverse range of chemotaxis trajectories.**

Key words: chemotaxis, orientation, locomotion, nematode, behavioral modeling, *Caenorhabditis elegans*.

Introduction

In a radial gradient of chemical attractant, wild-type nematodes *Caenorhabditis elegans* reach the gradient peak by moving almost directly up the gradient (Ward, 1973; Pierce-Shimomura et al., 1999). Statistical analysis of this behavior shows that movement down the gradient raises the probability of sharp turning events called pirouettes, and that movement up the gradient lowers the probability of pirouettes (Pierce-Shimomura et al., 1999). Pirouettes not only serve to stop the animal from moving down the gradient, they also reorient the animal up the gradient. Computer simulations of the pirouette mechanism have shown that it is sufficient to reproduce directed tracks like those of real worms.

Certain mutant strains exhibit chemotaxis trajectories that differ markedly from wild-type trajectories, raising the question of whether the pirouette mechanism is the only behavioral strategy for chemotaxis in *C. elegans*. One such strain is the so-called bent-head mutant (*unc-23*), in which the worm's head is permanently fixed at an angle to the main body axis because of a defect in muscle attachment (Fig. 1A; Ward, 1973; Waterson et al., 1980). In a radial gradient, bent-head mutants move up the gradient on a striking spiral trajectory centered on the gradient peak (Ward, 1973). Visual inspection of *unc-23* mutants suggests that the bent head acts like a rudder at the front of the worm, causing it to orbit in tight overlapping curls as it progresses along the spiral (Ward, 1973). Thus the chemotaxis trajectory of the *unc-23* mutant is complex and it is not immediately obvious whether such a track could be produced by a strategy as simple as the pirouette mechanism. Indeed, based on inspection of the tracks of *unc-23* and other mutants, an alternative to the pirouette mechanism has been proposed whereby the animal continually aligns its head with the direction of steepest ascent.

Here we use a combination of experiment and theory to show that the pirouette mechanism is sufficient to reproduce the spiral chemotaxis trajectory of *unc-23* mutants. We conclude that the pirouette mechanism explains a wider range of orientation trajectories than previously recognized.

Materials and methods

Animals

The strain *unc-23(e611)* was obtained from The *C. elegans* Genetics Center and raised as described by Brenner (1974). This allele was the same one used in the original study of the *unc-23* mutant (Ward, 1973). Mutants were grown at room temperature (19–24°C) in mixed-stage populations on agar-filled plates seeded with OP50 bacteria for food. The chemotaxis behavior of *unc-23* mutants was compared with

wild-type *C. elegans* (N2) from a previous study (Pierce-Shimomura et al., 1999). Wild-type worms (*N*=84) were raised identically to *unc-23* mutants (*N*=52) and tested in parallel. Analysis of this first data set is presented in Figs 1Bi,Biii,Biv,C,D and 2. A second set of *unc-23* mutants (*N*=10) was tested separately to compare with mutants from a previous study (Ward, 1973). Analysis of this second data set is presented in Figs 1Bii and 5A.

Chemotaxis assays and behavioral analysis

Animals were rinsed off food plates with assay medium and placed on a foodless, agar-filled holding plate for 0.5–2 h. The assay medium contained (in mmol l^{-1}): NH_4Cl 2, $CaCl_2$ 1, $MgSO_4$ 1, and KPO_4 25, pH 6.5. The agar in the holding plate contained only assay medium. Single adult hermaphrodites (1–3 days old) were then transferred to assay plates (diameter=9 cm, agar depth=0.264 cm) containing either a radial Gaussian-shaped gradient of the attractant ammonium chloride (NH_4Cl) (*N*=77) or a uniform concentration of NH_4Cl (*N*=57). The animal's centroid coordinates relative to the peak of the gradient were recorded with an automated tracking system that samples behavior at ~1 Hz as described previously (Pierce-Shimomura et al., 1999). The tracking system used an image analysis program (ImagePro Plus, Media Cybernetics, Silver Spring, MD, USA) to record the position of the animal and a computer-controlled motorized stage (Prior Scientific, Rockland, MA, USA) to reposition the animal within the field of view as necessary. Centroid coordinates and instantaneous velocity were used to calculate the estimated sensory input (rate of change of attractant concentration (*dC*/*dt*) at the animal's location), and the motor output (speed and turning rate) with equations described previously (Pierce-Shimomura et al., 1999). Bearing (*B*) was defined as the angle between the worm's instantaneous velocity vector and the vector pointing to the gradient peak. The times at which pirouettes were initiated were identified by an empirically tested algorithm based on the time series of turning rate values (Pierce-Shimomura et al., 1999). The probability of pirouette initiation (P_{piro}) was calculated by dividing the total number of pirouette initiation events by the total number of time samples in each assay. Turning bias θ_{bias} was defined as the absolute value of an animal's average instantaneous turning rate over the course of an assay, excluding periods during pirouettes.

Chemical gradients

Gradients were formed by adding drops of the attractant NH_4Cl to plates containing agar made from assay medium. Two different types of Gaussian gradients were used.

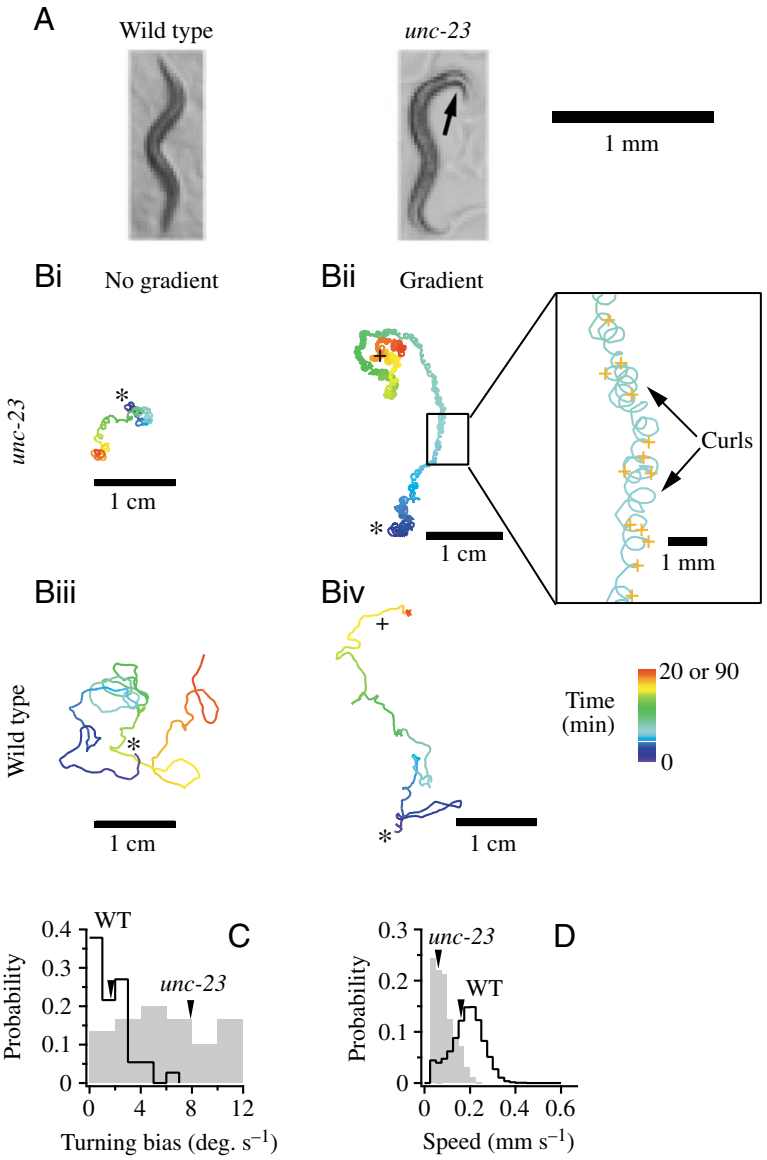

Fig. 1. Effect of the *unc-23* bent-head phenotype on movement. (A) Morphology of typical wild-type and *unc-23* worms. The bend in the head of the *unc-23* mutant is indicated by an arrow. (B) Comparison of dispersion and chemotaxis behavior for wild-type (Biii,Biv) and *unc-23* mutant (Bi,Bii) animals. Shown are representative tracks made by individual *unc-23* mutants and wild-type animals in the absence of a gradient (Bi,Biii) and in the presence of a radial gradient of chemical attractant (NH_4Cl; Bii,Biv). The *unc-23* track comprises a series of curls visible in the expanded inset. Note that the handedness of the curls, indicative of turning bias (clockwise), is opposite to the handedness of the spiral track (counterclockwise). Pirouette initiation events are indicated by orange crosses superimposed on the magnified track within the inset. Animals were started near asterisks; the gradient peak is indicated by the plus sign. Color represents time, as shown in the key. Elapsed time was 20 min for tracks Bi, Biii and Biv, and 90 min for the track in Bii. (C,D) Distributions of turning bias and instantaneous speed for wild-type (black lines) and *unc-23* mutant (solid gray bars) animals. Arrowheads indicate the average for each distribution.

The first type of gradient (Fig. 1Bii) was identical to the one used in the original study of the *unc-23* mutant (Ward, 1973).

This gradient was constructed by placing two 5 μl drops of 3 mol l^{-1} NH_4Cl at the center of the assay plate 12 and 3 h before the experiment. Concentration was estimated as 2–50 mmol l^{-1}, according to the diffusion equation for a point bolus in a thin slab (eqn 1 and 2 of Pierce-Shimomura et al., 1999; Crank, 1956).

The second type of gradient (Figs 1Biv,C,D, 2) was used to compare the chemotaxis behavior of *unc-23* mutants with a previously studied group of wild-type animals (Pierce-Shimomura et al., 1999) in which the gradient was formed by placing 2 drops of 0.5 mol l^{-1} NH_4Cl at the center of the plate 12 and 3 h before the experiment. Because *unc-23* mutants move slower than wild-type animals (Ward, 1973, and this study), they normally experience a restricted range of *dC/dt* values relative to wild-type animals assayed in identical gradients. Therefore, to ensure that *unc-23* mutants would experience a similar range of *dC/dt* values, we assayed them in a steeper gradient than the ones used for wild-type worms. Accordingly, the *unc-23* gradients were formed by placing two 5 μl drops of 1 mol l^{-1} NH_4Cl at the center of the plate 12 and 3 h before the experiment. Plotting histograms of values for *dC/dt*, we found that *unc-23* and wild-type worms assayed in these two gradients experienced similar ranges of *dC/dt* values between –0.05 and 0.05 mmol l^{-1} s^{-1}. Thus, any difference between pirouette behavior for the *unc-23* mutant and wild-type is less likely to be due to a difference in the range of *dC/dt* sensed and more likely to be due to an effect of the *unc-23* mutation.

Results

To study the locomotion of *unc-23* mutants, we used an automated tracking system to follow individual adult worms crawling on agar-filled plates. The agar contained either a uniform concentration of chemical attractant (2 mmol l^{-1} NH_4Cl) or a radial gradient of chemical attractant (NH_4Cl, range: 2–16 mmol l^{-1}).

In a uniform concentration of attractant, *unc-23* mutants made complex tracks consisting of overlapping curls that contrasted with the comparatively smooth tracks made by wild-type animals (Fig. 1Bi,Biii). Viewed from above, *unc-23* mutant animals with heads bent to the right made clockwise curls, whereas animals with heads bent to the left made counterclockwise curls. Thus the tendency to make curls is due to the bent-head phenotype, as reported (Ward, 1973). However, the severity of the bent-head phenotype varied considerably, ranging from animals with a profound bend that made tight (small radius) curls to animals with no visible bend that did not make curls (data not shown). We quantified this variability in terms of each animal's turning bias, computed as the animal's average instantaneous turning rate over a 20 min observation period. Turning bias histograms are shown in Fig. 1C for *unc-23* mutants and wild-type worms. The *unc-23* distribution was shifted toward larger biases relative to the wild-type distribution. We also quantified the effect of the bent head on average instantaneous speed; *unc-23* mutants were approximately 2.5 times slower than wild-type animals (Fig. 1D). Thus the two main effects of the *unc-23* mutation on locomotion are to increase the range of turning biases between individuals and reduce speed.

In the case of a radial gradient, we found that some *unc-23* individuals made spiral tracks (Fig. 1Bii) as previously reported (Ward, 1973), whereas others did not. We found that we could predict whether or not an *unc-23* worm would make a spiral track in a gradient by first observing the diameter of the worm's curls in the absence of a gradient. Only those worms whose curls measured 0.5–1.0 mm in diameter consistently made spiral tracks. Within this range of diameters, the worm's body occupies approximately one-third to two-thirds of the circumference of a curl. Worms whose curl diameter was below this range made little or no progress up the gradient, whereas worms whose curl diameter was above this range reached the gradient peak without making spirals, i.e. their tracks were essentially wild-type in shape (data not shown). These results indicate that the likelihood of a spiral track depends on the severity of the bent-head phenotype.

Because the tracks of *unc-23* mutants with bent heads were so different from the tracks of wild-type animals, it was unclear whether the pirouette mechanism operates in this strain. We have shown previously that the probability of pirouette initiation (P_{piro}) in wild-type animals is related to the rate of change of attractant concentration (*dC/dt*) at the animal's location as it moves in the gradient (Pierce-Shimomura et al., 1999). P_{piro} is higher than baseline probability when the animal moves down the gradient (facilitation for $dC/dt<0$) and lower than baseline probability when the animal moves up the gradient (suppression for $dC/dt>0$). Although the points of pirouette initiation were difficult to discern within the *unc-23* tracks because of their overlapping curls, these points were easy to detect automatically with an algorithm based on the time series of instantaneous turning rate values (example Fig. 1Bii inset). To test whether facilitation and suppression are regulated by *dC/dt* in *unc-23* mutants as in wild-type animals, we plotted P_{piro} as a function of *dC/dt* for wild-type and *unc-23* mutants tested in a gradient (Fig. 2A). These data were compared against separate groups of wild-type and mutant animals tested in the absence of a gradient to measure baseline levels of P_{piro}. We found that P_{piro} in *unc-23* mutants exhibited both facilitation and suppression relative to the basal P_{piro} as a function *dC/dt* similar to the facilitation and suppression seen in wild type. We conclude that a pirouette mechanism operates in *unc-23* mutants.

We next asked whether pirouettes are initiated normally in *unc-23*. This was done by plotting the distribution of orientations relative to the gradient peak immediately before pirouettes for the wild-type and *unc-23* mutant animals. Orientation was defined in terms of bearing (B) relative to the peak of the gradient, where $B=0°$ means movement directly up the gradient and $B=\pm180°$ means movement directly down the gradient. Surprisingly, the distributions of B before pirouettes (B_{before}) for the two strains were statistically indistinguishable [Fig. 2B; Watson-Williams test (Zar, 1984): $F_{1,1953}=2.18$,

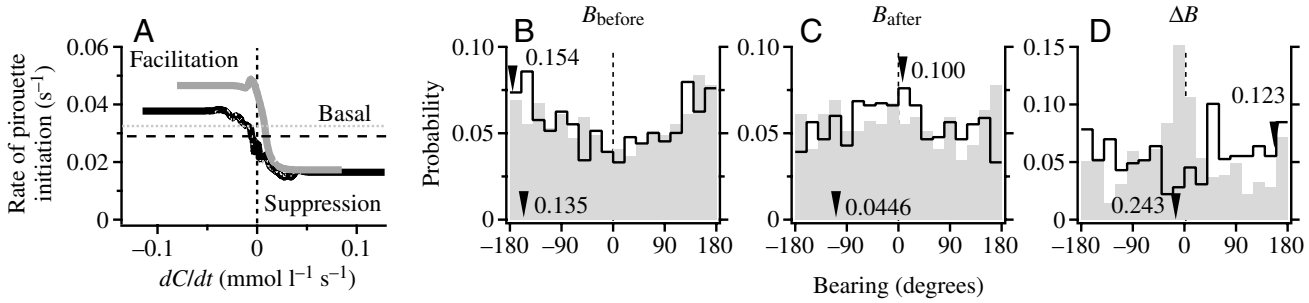

Fig. 2. Analysis of pirouette initiation and execution. (A) Instantaneous pirouette rate as a function of the value of dC/dt for wild-type and mutant animals in NH_4Cl gradients. The data have been smoothed with a box filter (4001 points long). The gray line represents *unc-23* data (21 293 points); the black line represents wild-type data (29 171 points). Spontaneous or basal pirouette rates measured in the absence of a gradient are represented by horizontal lines (black broken line, wild-type; gray dotted, *unc-23*). (B–D) Histograms of bearings immediately before pirouettes (B), immediately after pirouettes (C), and changes in bearing (D) for the animals in A. The wild-type distributions (black lines) contain 1129 pirouettes; the *unc-23* distributions (solid gray bars) contain 816 pirouettes. Arrowheads indicate the angle of the vector average for each distribution; numbers indicate the corresponding vector magnitude.

P=0.14]. The similarity of the wild-type and *unc-23* B_{before} distributions could have arisen because we happened to select *unc-23* worms with a mild phenotype. This explanation seems unlikely, however, because the *unc-23* B_{before} distribution was computed for the same sample of mutant worms shown in Fig. 1C, which contains a significant number of individual worms with a severe turning bias phenotype. Thus, *unc-23* pirouettes are initiated normally in *unc-23* mutants despite the fact that the head is bent.

In wild-type animals, the average effect of a pirouette is to reorient the animal up the gradient (Pierce-Shimomura et al., 1999). To determine whether pirouettes could also reorient *unc-23* mutants normally, we compared the distribution of bearings immediately after pirouettes (B_{after}) for wild-type and *unc-23* mutant animals. The wild-type B_{after} distribution had a peak at 0°, whereas the *unc-23* distribution was essentially flat [Fig. 2C; modified Rayleigh test (Zar, 1984): z=0.906, d.f.=1128, P>0.20]. Thus, pirouettes did not reorient the *unc-23* mutants up the gradient as they did for wild-type animals. This observation was reinforced by the distribution of changes in bearing (ΔB) produced by individual pirouettes in the two strains (Fig. 2D). The wild-type ΔB distribution had a minimum near 0° and a broad peak near ±180°, indicating that most pirouettes produced relatively large changes in bearing. In contrast, the *unc-23* ΔB distribution had only a minor peak near ±180° and a major peak at 0°, indicating that the most common type of pirouette produced little or no change in direction, rather than a 180° change in direction as in wild-type worms. Thus a key defect in the *unc-23* pirouette mechanism is the tendency to continue moving in the same direction after a pirouette. This defect is consistent with the anatomical finding of head muscle attachment defects in *unc-23* mutants (Waterson et al., 1980), because such a defect could limit a worm's ability to make large course corrections.

We next considered how spiral tracks might be generated by *unc-23* mutants. Ward (1973) suggested that *unc-23* spirals result from the tendency to align the head up the gradient, coupled with the ruddering effect of the head bend. However, the fact that *unc-23* exhibits pirouettes triggered specifically by movement down the gradient suggests an alternative explanation. Perhaps the spiral track is due to pirouettes triggered when the worm moves along the down-gradient segment of the curl. To test this idea, we created a mathematical model of *unc-23* chemotaxis behavior.

Worms were represented in the model as a point that moved with real-worm statistics in a virtual gradient. The virtual gradient was the same as the real gradient used in the experiments of Fig. 1Bii. At each time point t in the simulation (Δt=1 s), the worm's location (x_t, y_t) and direction θ_t in the virtual gradient were updated according to the equations:

$$\theta_{t+1}=\theta_t + \Delta t\theta_{bias} ,$$

$$x_{t+1}=x_t + v\cos(\theta_t) ,$$

$$y_{t+1}=y_t + v\sin(\theta_t) ,$$

where θ_{bias} is turning bias and v is instantaneous speed. To explore the effect of turning bias on track trajectory, a single value for θ_{bias} was randomly selected for each model worm from a range of values (6–12 deg. s^{-1}) consistent with the subset of the distribution obtained from tracking data of real *unc-23* animals that did not overlap with wild-type values (Fig. 1C). Speed for each model worm was constant and set to the average speed from the distribution obtained from real animals (0.07 mm s^{-1}; Fig. 1D). Each model worm made pirouettes probabilistically according to the instantaneous value of P_{piro}, updated for each time point according to the empirically derived relationship between dC/dt and P_{piro} shown in Fig. 2A. When a pirouette occurred, direction was updated for that time step by sampling randomly from the ΔB distribution of Fig. 2D. Model worms were started 35 mm away from the center of the radial gradient with a random initial direction and allowed to move for the equivalent of 90 min.

We found that simulations of *unc-23* pirouette behavior always reproduced the overall spiral shape of chemotaxis tracks of the *unc-23* mutant for θ_{bias} values in the range

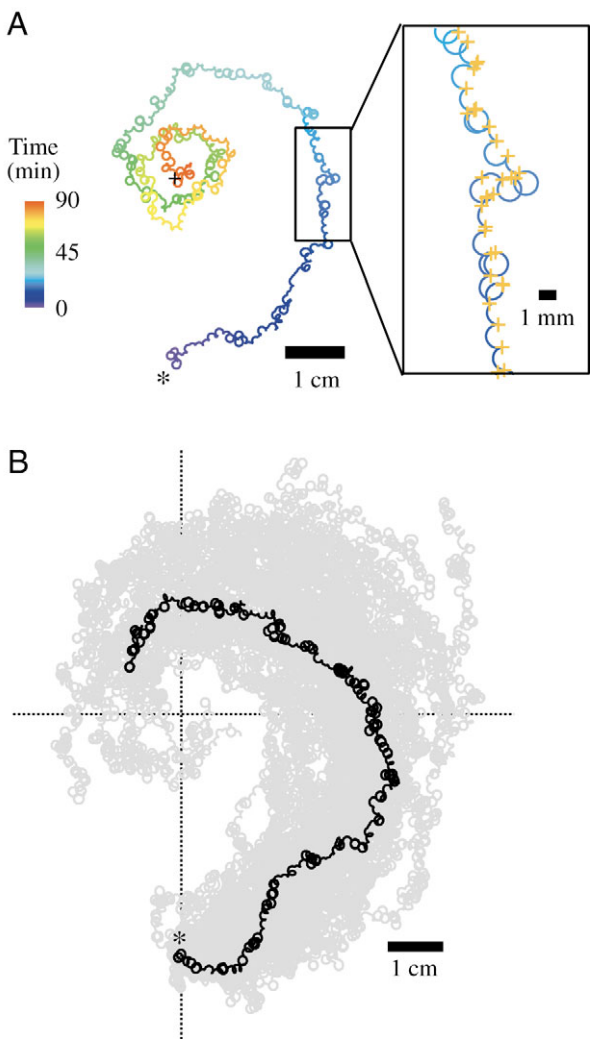

Fig. 3. Mathematical model of *unc-23* behavior. (A) Representative track of a simulated *unc-23* mutant in a radial gradient. Note that the simulated worm had a clockwise turning bias (7 deg. s^{-1}) and made a counterclockwise spiral, as do real *unc-23* mutants (Fig. 1Bii). The gradient peak is indicated by the plus sign. Color represents time (see color scale). Pirouette initiation events are indicated by orange crosses superimposed on the magnified track within the inset. (B) Population behavior of simulated *unc-23* worms in a radial gradient. The track of one simulated worm is highlighted in black; all other tracks are gray (*N*=50). Each simulated worm had a right-handed turning bias and made a left-handed spiral. The gradient peak is indicated by intersection of dotted lines. Simulations in A and B were started near the asterisks.

6–12 deg. s^{-1}. Like the real *unc-23* mutants, model worms advanced up the gradient in a spiral track composed of a series of overlapping curls (Fig. 3A,B). Points in the track where pirouettes occurred were evident by truncated curls, usually at a point where the track curled down the gradient (crosses superimposed on the magnified track in Fig. 3A). Thus, the pirouette mechanism is sufficient to account for spiral-shaped chemotaxis tracks in a model that contained no free parameters.

The *unc-23* simulation also reproduced a key detail concerning the handedness of the spiral tracks of real *unc-23* chemotaxis. Inspection of the tracks of those real *unc-23* worms that spiralled (i.e. those that had a curl diameter between 0.5–1.0 mm) revealed a consistent relationship between the handedness of the turning bias and the handedness of the spiral; in 10 out of 10 cases, the handedness of the bias and spiral were opposite. We found the same relationship in the model. For instance, the simulation shown in Fig. 3A had a clockwise turning bias and made a counterclockwise spiral. Moreover, all runs of the simulation (*N*=50) made tracks with this relationship (Fig. 3B). Thus, although the pirouette mechanism is conceptually simple, it appeared to predict the chemotaxis behavior of real *unc-23* mutants in terms of both the overall spiral track and the relationship between the handedness of the spiral relative to the handedness of the bias.

Our observation that the animal's turning bias and spiral track have opposite handedness appeared to conflict with the original observations of the *unc-23* mutants in which the handedness of the turning bias and spiral were reported to be the same (Ward, 1973). This apparent conflict raised the possibility that animals from the two studies may have used different chemotaxis strategies. We have found, however, that a simple geometrical analysis of *unc-23* pirouette behavior provides a way to reconcile these different observations.

Consider the case of an *unc-23* worm with a significant turning bias and a simplified pirouette behavior such that pirouettes result in direction changes of either 0 or 180°. These angles correspond to the two maxima in the *unc-23* ΔB distribution of Fig. 2D. Simplifying pirouette behavior in this way is valid because the angles intermediate between 0 and 180° occur in complementary pairs (e.g. +90° and –90°), whose effects cancel out over the long term. Such a worm will move along a circular path punctuated by occasional pirouettes. Pirouettes of 0° have no effect, so the worm stays on its circular course. In contrast, pirouettes of 180° cause the worm to embark on a new circular trajectory, tangent to the original one at the point where the pirouette occurred. Because pirouette initiation depends probabilistically on the history of dC/dt (Dusenbery, 1980; Pierce-Shimomura et al., 1999; Miller et al., 2005), pirouettes will occur with variable latency with respect to the instant at which the animal enters the down-gradient half of its circular trajectory. Thus pirouettes can occur in each of the four quadrants shown in Fig. 4. The relative frequency of pirouettes in the four quadrants will depend on such factors as the speed of the worm and the steepness of the gradient, but for now let us consider the simple case in which pirouettes occur with a fixed latency such that they always occur in the same quadrant (I, II, III or IV).

For the case where pirouettes occur with the shortest latency (quadrant I pirouettes) the track spirals toward the peak (positive chemotaxis) with a handedness that is opposite to the handedness of the turning bias (Fig. 4B). This track corresponds to the *unc-23* tracks reported here (e.g. Fig. 1Bii). Pirouettes occurring with longest latency (quadrant IV pirouettes) also yield positive chemotaxis, but now the

handedness of the spiral is the same as the handedness of the turning bias (Fig. 4A). This track corresponds to the tracks reported in the original study (Ward, 1973). Pirouettes occurring with intermediate latencies (quadrants II and III pirouettes) yield tracks that spiral away from the peak (negative chemotaxis; Fig. 4C,D). Such tracks have not been reported for *unc-23* mutants. The fact that the pirouette mechanism can generate spiral tracks with positive chemotaxis and either type of handedness provides a possible reconciliation of the present study and the original one. For example, it is conceivable that in the original study, worms were observed in regions where the gradient was less steep than in the present study, resulting in more quadrant IV pirouettes than quadrant I pirouettes.

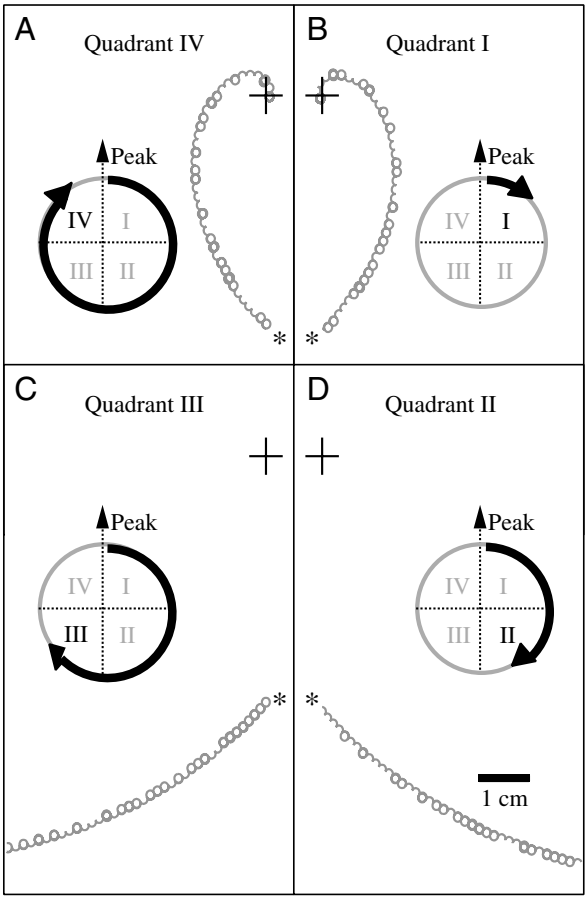

Fig. 4. Geometric analysis of the interaction between *unc-23* pirouette behavior and turning bias. An idealized *unc-23* mutant animal moves with a constant clockwise turning bias and produces pirouettes with either a 180° or 0° change in bearing. The animal moves in a radial gradient from the starting position indicated by asterisks; the gradient peak is at the plus sign. Shown are four cases in which the animal initiates pirouettes in only one quadrant (I, II, III or IV) that is defined relative to direction of the gradient peak (see diagrams adjacent to each track). (A) Quadrant IV pirouettes produce a clockwise spiral track. This type of track corresponds to the *unc-23* tracks reported in the original study (Ward, 1973). (B) Quadrant I pirouettes produce a counterclockwise spiral track centered on the radial gradient peak. This type of track corresponds to the real *unc-23* track shown in Fig. 1Bii. (C,D) Quadrants II or III pirouettes produce spiral tracks leading down the gradient away from the gradient peak.

Does the simplified geometric analysis apply to the chemotaxis tracks of real worms, in which pirouettes occur with a variable latency? In the case of variable latency, the geometric analysis predicts that for positive chemotaxis with opposite spiral-bias handedness, pirouettes in quadrant I should dominate. To test this prediction, we examined the relative frequency of pirouettes in quadrants I–IV for our *unc-23* worms, all of which exhibited spiral tracks with opposite spiral-bias handedness. As predicted by the geometric analysis, the most frequent pirouettes were those in quadrant I (Fig. 5A). We conclude that the geometric analysis is consistent with the behavior of real *unc-23* worms in our assay.

As a further test of the geometric analysis in the case of variable pirouette latency, we asked whether the frequency of pirouettes observed for real worms in each quadrant was sufficient to produce a spiral track with opposite spiral-bias handedness in a simulated worm. We did this by noting the time at which the simulated worm entered the down-gradient region of its circular trajectory and, at that point, randomly selecting one of four latencies according to the probabilities dictated by the observed frequencies of quadrant I–IV pirouettes shown in Fig. 5A. Overall pirouette rate was adjusted to match the average pirouette rate in real *unc-23* worms ($0.04\ s^{-1}$; Fig. 2A). The simulated worm's direction after a pirouette was updated by sampling randomly from the ΔB distribution of Fig. 2D. Because of the stochastic nature of the model, we ran 50 simulated worms for the equivalent of 90 min each. We found that all of the simulated worms exhibited spiral tracks with opposite spiral-bias handedness (representative track in black and all others tracks in gray in Fig. 5B). This result provides additional support for the geometrical analysis.

Discussion

We sought to determine whether the pirouette mechanism is sufficient to explain the spiral-shaped chemotaxis tracks made by the *C. elegans* bent-head mutant *unc-23*. A tracking analysis of individual *unc-23* animals showed that the head bend does not interfere with pirouette initiation, but profoundly disrupts pirouette execution. A mathematical model of *unc-23* pirouette behavior showed that the pirouette mechanism could account for the spiral tracks. Because we find that the pirouette mechanism is sufficient to produce spiral tracks, no additional behavioral strategy need be evoked to explain the unusual tracks of the *unc-23* mutants.

Our tracking analysis confirms and extends many of the main observations of the initial report on *unc-23* chemotaxis behavior (Ward, 1973). In agreement with previous results (Ward, 1973), we found that whereas some *unc-23* individuals had a wild-type turning bias, other *unc-23* individuals had a strong turning bias imposed by their bent head. For individuals with a bent head, the head appeared to act like a rudder that forces the mutant to move in a curling path. In an extension of

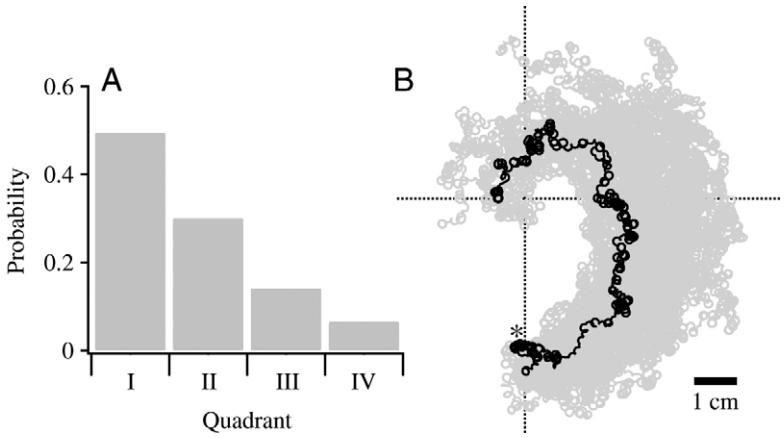

Fig. 5. The variability of pirouette latency within curls and its affect on the *unc-23* model. (A) Pirouette probability by quadrant in real *unc-23* worms. Quadrants I–IV are defined as in Fig. 4. Total number of pirouettes was 216. (B) Population behavior of simulated *unc-23* worms that initiate pirouettes according to the probabilities in A. Imposing the probabilities in A on the model was sufficient to produce spiral tracks with opposite spiral-bias handedness. Simulated worms had a constant clockwise turning bias of 7 deg. s^{-1}. Each simulated worm was started near asterisks and allowed to move for the equivalent of 90 min. The gradient peak is indicated by intersection of dotted lines. The track of one simulated worm is highlighted in black; all other tracks are gray (*N*=50).

the earlier work, we found that the likelihood of spiral tracks depends on the severity of the head bend. Only those individuals with a moderate turning bias made spiral tracks; individuals with a weak turning bias did not make spiral tracks, whereas individuals with a severe turning bias made little progress away from the starting location.

Our analysis also revealed a key difference from the initial study of the *unc-23* mutant (Ward, 1973). We found that all animals (10 out of 10) made tracks that had the opposite relation between the handedness of the spiral track and the handedness of the turning bias. This seemed to conflict with the initial study, which reported that the handedness of the spiral and the handedness of the turning bias were the same (Ward, 1973). However, we found that we could resolve this conflict by considering how the latency of pirouettes interacts with turning bias to produce spirals with the same or opposite handedness. A geometric consideration of this interaction showed that it could yield tracks like those in the original study, in which the spiral and turning bias had the same handedness, or tracks like those in the present study, in which the spiral and turning bias had opposite handedness.

The results reported here revise our assessment of the main chemotaxis strategy in *C. elegans*. Based on qualitative inspection of the tracks that wild-type and mutant animals left in an agar substrate, Ward (1973) proposed that a worm adjusts the extent of dorsal *vs* ventral body bends so as to minimize the difference in the attractant concentration sensed on either side, somewhat like a weathervane shifting in the wind. The weathervane strategy was proposed as the primary mechanism to explain the relatively direct tracks made by wild-type animals and the spiral tracks of the *unc-23* mutant. However, we find that the pirouette mechanism can explain both the elementary and higher-order features of chemotaxis behavior in wild-type and *unc-23* animals without appeal to alternatives. We therefore propose that the pirouette mechanism is the primary strategy for *C. elegans* chemotaxis in laboratory assays, and that other mechanisms, including a possible weathervane strategy, serve as secondary or alternative strategies.

The authors thank Tod Theile and Steven Augustine for photography, and members of the Lockery lab, Hongkyun Kim and Matt Schreiber for critical review. This work was supported by grants from the National Science Foundation, the National Institute of Mental Health, the National Heart, Lung and Blood Institute, the Office of Naval Research, The Sloan Foundation, The Searle Scholars Program and National Institutes of Health predoctoral fellowship Training Grant GM07257. Worms were provided by the *Caenorhabditis* Genetics Center, which is funded by the National Institutes of Health National Center for Research Resources.

References

Brenner, S. (1974). The genetics of *Caenorhabditis elegans*. *Genetics* **77**, 71-94.

Crank, J. (1956). *The Mathematics of Diffusion*. Oxford: Clarenden.

Dusenbery, D. (1980). Responses of the nematode *Caenorhabditis elegans* to controlled chemical stimulation. *J. Comp. Physiol. A* **136**, 327-331.

Miller, A., Thiele, T., Faumont, S., Moravec, M. and Lockery, S. (2005). Step-response analysis of chemotaxis in *Caenorhabditis elegans*. *J. Neurosci.* **13**, 3369-3378.

Pierce-Shimomura, J., Morse, T. and Lockery, S. (1999). The fundamental role of pirouettes in *Caenorhabditis elegans* chemotaxis. *J. Neurosci.* **19**, 9557-9569.

Ward, S. (1973). Chemotaxis by the nematode *Caenorhabditis elegans*: identification of attractants and analysis of the response by use of mutants. *Proc. Natl. Acad. Sci. USA* **70**, 817-821.

Waterston, R., Thomson, J. and Brenner, S. (1980). Mutants with altered muscle structure in *C. elegans*. *Dev. Biol.* **77**, 271-302.

Zar, J. (1984). *Biostatistical Analysis*. Englewood Cliffs, NJ: Prentice-Hall.